AD-A049 057 NAVAL RESEARCH LAB WASHINGTON D C F/G 4/1
LOW ALTITUDE PLASMA LINE ANISOTROPY.(U)
OCT 77 E S ORAN, P J PALMADESSO
UNCLASSIFIED NRL-MR-3584 SBIE-AD-E000 086 NL

| OF |
AD
A049057

END
DATE
FILMED
2-78
DDC

(12)

adw0000086

NRL Memorandum Report 3584

(6)

Low Altitude Plasma Line Anisotropy.

(10) Elaine S. Oran and Peter J. Palmadesso

Plasma Physics Division
Naval Research Laboratory
Washington, D.C. 20375

and

Suman Ganguly

National Astronomy and Ionosphere Center
Arecibo Observatory
Arecibo, Puerto Rico 00612

(14) NRL-MR-3584

(9) Interim rept.,

(11) Oct 77

(12) 19 p.

(18) SBIE

(19) AD-E000 086

NAVAL RESEARCH LABORATORY
Washington, D.C.

251 950

SECURITY CLASSIFICATION OF THIS PAGE (When Data Entered)

REPORT DOCUMENTATION PAGE

READ INSTRUCTIONS BEFORE COMPLETING FORM

1. REPORT NUMBER: NRL Report 3584
2. GOVT ACCESSION NO.:
3. RECIPIENT'S CATALOG NUMBER:

4. TITLE (and Subtitle): LOW ALTITUDE PLASMA LINE ANISOTROPY

5. TYPE OF REPORT & PERIOD COVERED: Interim report on a continuing NRL Problem.

6. PERFORMING ORG. REPORT NUMBER:

7. AUTHOR(s): E. S. Oran and P. J. Palmadesso, NRL, and Suman Ganguly, Arecibo Observatory

8. CONTRACT OR GRANT NUMBER(s):

9. PERFORMING ORGANIZATION NAME AND ADDRESS: Naval Research Laboratory, Washington, D. C. 20375

10. PROGRAM ELEMENT, PROJECT, TASK AREA & WORK UNIT NUMBERS: NRL Problem No. A03-30

11. CONTROLLING OFFICE NAME AND ADDRESS: Office of Naval Research, 800 North Quincy Street, Arlington, VA 22217

12. REPORT DATE: October 1977

13. NUMBER OF PAGES: 18

14. MONITORING AGENCY NAME & ADDRESS (if different from Controlling Office):

15. SECURITY CLASS. (of this report): UNCLASSIFIED

15a. DECLASSIFICATION/DOWNGRADING SCHEDULE:

16. DISTRIBUTION STATEMENT (of this Report)

Approved for public release; distribution unlimited.

17. DISTRIBUTION STATEMENT (of the abstract entered in Block 20, if different from Report)

18. SUPPLEMENTARY NOTES

19. KEY WORDS (Continue on reverse side if necessary and identify by block number)

Plasma lines
Photoelectrons
Ionosphere
Incoherent scatter

20. ABSTRACT (Continue on reverse side if necessary and identify by block number)

Plasma line observations obtained from incoherent radar backscatter have been used as a ground-based method for deriving information about the size and anisotropy of the ionospheric photoelectron fluxes. In the past data interpretation has been confined to altitudes above the F2 peak. Measurements below the F2 peak consistently show an anisotropy in the ratio of the downshifted to upshifted amplitudes of 20-50% when it is generally assumed that diffusion processes dominate. We describe calculations of the plasma line intensity which use a multi-angle multi-energy calculation of the

are described

(Continued)

DD FORM 1 JAN 73 1473 EDITION OF 1 NOV 65 IS OBSOLETE S/N 0102-LF-014-6601

20. (Continued)

photoelectron distribution function. The calculated electron flux exhibits a low altitude, low energy anisotropy which is reflected in the plasma line measurements. Given anisotropic elastic electron-neutral cross-sections, the flux anisotropy arises when the local mean free path is of the order of the local scale height. The net effect is conversion of a spatial density in homogeneity into a velocity distribution anisotropy.

CONTENTS

LOW ALTITUDE PLASMA LINE ANISOTROPY

INTRODUCTION

Plasma line observations obtained from incoherent radar backscatter have been used as a ground-based method for deriving information about the size and anisotropy of the ionospheric photoelectron fluxes. In the past, interpretation of plasma line data has been confined to altitudes above the F2 peak where plasma lines enhanced by photoelectrons moving upward have larger amplitudes than those enhanced by downward moving photoelectrons. The net upward electron flux in the topside ionosphere arises because the photoelectron mean free path is large and within a mean free path, more electrons are produced just below a given point of observation than just above it.

At lower altitudes the photoelectron mean free path is small compared to the gradient scale length of the photoelectron production rate, yet plasma line anisotropy is still observed. Measurements below the peak were first shown by Yngvesson and Perkins (1968) and recently by Legeune and Kofman (1977). These observations have consistently shown anisotropy in the plasma line amplitude ranging from 20% to a factor of two for upgoing to downgoing particles. Measurements made at Arecibo have shown a 20-50% anisotropy.

In this paper we describe calculations of the plasma line intensity which use a detailed transport equation solution for the photoelectron distribution function. We postulate from the work described below that the observed low altitude anisotropy reflects the forward peaked property of the elastic electron neutral scattering cross sections. We further argue that given

Manuscript submitted August 8, 1977.

anisotropic cross sections, an anisotropy in the low altitude electron fluxes arises when the local mean free path is of the order of the local scale height.

LOW ALTITUDE FLUX ANISOTROPY

The photoelectron transport calculation used in our plasma line studies has been described in Oran and Strickland (1976). Further technical description of the general method can be found in Strickland *et al.* (1976). Figures 1 and 2 show results of a typical calculation of the photoelectron flux as a function of pitch angle at 157 and 355 km for selected energies. Figure 3 shows the way in which the calculated flux anisotropy of 4 ev electrons varies with altitude.

The low altitude, the low energy flux anisotropy shown in Figures 1 and 3 arises as a consequence of the fact that the mean free path of an energetic photoelectron (E > 10 ev) can be of the same order of magnitude as the local neutral density scale height. This fact, coupled with an anisotropy in the elastic electron-neutral collision cross sections, results in a net downward flow of particles. The cross sections for atomic oxygen, which are shown in Figure 4 (Blaha and Davis, 1975), show a typical angular dependence: they are forward peaked and reach a minimum at some angle greater than ninety degrees.

Some insight into the nature of this low altitude flux anisotropy can be obtained by looking at a simplified photoelectron calculation based on the limiting case in which electron-neutral collisions are assumed to be entirely forward scattered. We take the photoelectron equation of motion to be

$$\dot{v} = -\nu_{en}(z)v \tag{1}$$

where ν_{en} is the electron-neutral collision frequency and z is the spatial coordinate in the vertical direction. Then we consider a neutral gas in one dimension with a density gradient such that

$$\nu_{en}(Z) = \nu_o e^{-z/L}, \tag{2}$$

where L is the neutral density scale height. We then wish to solve an equation of the form

$$v \frac{\partial F_p}{\partial z} - \nu_{en} v \frac{\partial F_p}{\partial v} = \beta \delta (v \pm v_o), \tag{3}$$

which represents a steady state one dimensional Boltzmann equation for the distribution function, F_p, with a source of electrons at velocity $\pm v_o$. We assume that the electrons move through a medium in which their mean free path is very small compared to the gradient scale length of their production rate. This assumption is valid in the atmosphere up to about 200 km and allows us for the purposes of this discussion to set β equal to a constant

The solution to Eq. (3) is

$$F_p^{\pm}(v,z) = \frac{\beta}{v_o \left\{ \nu_o + \left[\pm v_o - v - \int_o^z \nu_{en}\, dz'/L \right] \right\}} \tag{4}$$

where ν_o is the collision frequency at $z = 0$. The superscripts on f_p, + and −, denote upgoing and downgoing particles, respectively. With no loss of generality we can define the altitude of interest to be $z = 0$, and Eq. (4) becomes

$$f_p^{\pm}(v,o) = \frac{\beta}{[\nu_o - (v \mp v_o)/L]}, \tag{5}$$

which is valid when $(\nu_o L - v_o) > 0$. This condition guarantees that electrons created at $z = \infty$ cannot reach $z = 0$. Violation of this constraint leads to a singularity in f_p^-, since β does not vanish at ∞ in this simple model. We define an anisotropy parameter

$$A(|v|) = \frac{f_p^-(|v|)}{f_p^+(|v|)} = \frac{\nu_o + (v_o - |v|)/L}{\nu_o - (v_o - |v|)/L}. \tag{6}$$

Note that there is no anisotropy when $|v| = v_o$ since $A(v_o) = 1$. The anisotropy builds up as the electron energy degrades.

In order to concentrate specifically on the low energy particles, we define the local mean free path as $L^{mfp} \equiv v_o/\nu_o$, so that when $L^{mfp}/L < 1$,

$$A(|v| << v_o) \simeq \frac{1 + L^{mfp}/L}{1 - L^{mfp}/L} \tag{7}$$

which shows that a significant anisotropy exists at low energies when the local photoelectron mean free path is comparable to the scale height. For example, from Figure 5 we see that this condition is satisfied for 10 ev electrons at 150 km.

We emphasize that Equation 7 is the result of a qualitative calculation given to help understand the detailed simulation results shown in Figures 1, 2, and 3. Aside from the unrealistic source term, Equation 3 includes *only* forward scattering with no diffusion effects. Thus it *overemphasizes* the anisotropy. The detailed simulation is a solution of the steady state Boltzmann equation

$$v \frac{\partial F}{\partial z} + \dot{v} \cdot \nabla_v F = Q(z,v,t) + \frac{\partial F}{\partial t}\Big|_c, \tag{8}$$

where Q is a local source term, $\dot{v} \cdot \nabla_v F$ represents the loss of energy by the photoelectrons to the ambient electrons through collisions and plasma wave excitations, and $\partial F / \partial t|_c$ involves the details of elastic and inelastic collisions among electrons and neutral species. Solution of Equation (8) involves following the detailed degradation of the primary electron spectrum produced by ionization due to solar radiation and yields the distribution function, $F(z,v,\mu)$ where μ is the pitch angle (Oran and Strickland, 1976).

PLASMA LINES FROM INCOHERENT RADAR SCATTER

When the radar wavelength, λ, is very much larger than the Debye length, the radar signal is scattered incoherently by electron density fluctuations. Because the ionosphere is a non-equilibrium plasma, the intensity of the electron density fluctuations is enhanced beyond that expected from purely thermal fluctuations. The fast photoelectrons feed energy into and

excite the plasma waves which in term are Landau damped. The total amplitude of the plasma line signal represents an equilibrium between a number of processes which excite and damp the plasma waves scattering the radar beam. Collisions between thermal electrons and ions can excite plasma waves and the interaction with energetic photoelectrons can enhance the signal smplitude above the thermal equilibrium value. The waves are damped by electron collisions with ions and neutrals as well as by Landau damping.

The plasma line signal amplitude can be expressed in terms of a temperature, T_p, which reduces to T_e when the plasma is in thermal equilibrium. The upshifted (downshifted) signal is a result of scattering off of plasma waves excited by electrons moving primarily down (up) the magnetic field line. Thus the returned signals, proportional to T_p^+ and T_p^-, may differ by an amount related to the degree of anisotropy in the photoelectron flux spectrum. The balance of processes exciting and damping the plasma waves leads to an expression for T_p,

$$\frac{T_p(v_\phi)}{T_e} = \frac{\chi^{ei} + f_p + f_{mb}}{\chi^{ei} + f_{mb} + L_p}, \tag{9}$$

(Perkins and Salpeter, 1965a and b). In this equation f_{mb} and f_p are the Maxwellian and photoelectron contributions to the plasma line source term and χ^{ei} represents the effects of electron collisions with ions and neutrals. The scattering occurs off of plasma oscillations of wavelength $\lambda/2$ and phase velocity $v_\phi = \nu_R \lambda/2$ and $E_\phi = \frac{1}{2} m_e v_\phi^2$. The returned plasma line signal is Doppler shifted about the radar frequency by an amount $\pm\nu_R$, where

$$\nu_R^2 = \nu_p^2 + \frac{12kT_e}{\lambda^2 m_e} + \nu_{ce}^2 \sin\theta \simeq \nu_p^2, \tag{10}$$

where ν_p is the plasma frequency, m_e is the electron mass, ν_{ce} is the electron cyclotron frequency, and θ is the angle between the direction of radar beam propagation and the magnetic field.

In the presence of the earth's magnetic field,

$$f_{mb} = \frac{N_e}{\cos\theta}\left(\frac{m_e}{2kT_e}\right)^{1/2} \sum_{n=-\infty}^{\infty} e^{-b\sin^2\theta} I_n(b\sin^2\theta)\, e^{-(y-n)^2/2\cos^2\theta} \tag{11}$$

(Salpeter, 1961), where N_e is the ambient electron density, I_n is the Bessel function of imaginary argument,

$$y = \nu_R/\nu_{ce}, \tag{12}$$

$$b = \frac{kT_e}{m_e}\frac{4}{\lambda^2\nu_{ce}^2}, \tag{13}$$

$$f_p(v_\phi) = \frac{2\pi}{\cos\theta} \sum_{n=-\infty}^{\infty} \int_{v_{min}}^{\infty} v_\perp J_n^2(W) F(v_\perp, u_n)\, dv_\perp, \tag{14}$$

(Fremouw *et al.*, 1969), where J_n is the Bessel function of real argument,

$$W = \frac{2\, v_\perp \sin\theta}{\lambda\, \nu_{ce}}, \tag{15}$$

$$u_n = \frac{\lambda(\nu_R - n\nu_{ce})}{2\cos\theta}. \tag{16}$$

The $v_\perp$ and u are the components of electron velocity perpendicular and parallel to the magnetic field, and $F(v_\perp, u)$ is the three-dimensional velocity distribution function for electrons where u is evaluated at u_n. The lower unit of the integral, v_{min}, corresponds to that velocity at which the photoelectron distribution function begins to deviate substantially from Maxwellian. The photoelectron contribution to the damping, L_p, can be expressed as

$$L_p = \frac{2\pi kT_e}{y\cos\theta} \sum_{n=-\infty}^{\infty} \int_{v_{min}}^{\infty} v_\perp J_n^2(W) \left\{\left[\frac{(y-n)}{m_e u}\frac{\partial}{\partial u} + \frac{n}{m_e v_\perp}\frac{\partial}{\partial v_\perp}\right] F(v_\perp, u)\right\}_{u=u_n} dv_\perp. \tag{17}$$

Substitution of a Maxwellian distribution function into f_p and L_p both yield f_{mb}. The χ^{ei} in Equation (9) is related to the electron-ion and electron-neutral collision frequencies by

$$\chi^{ei} = \frac{N_e}{\nu_p \alpha^3 \pi^3}\sqrt{\frac{m_e}{kT_e}}\,\nu_{ei}, \tag{18}$$

$$\alpha = \lambda/4\pi D \tag{19}$$

where D is the Debye length.

The plasma line is in thermal equilibirum, $T_p = T_e$, when either thermal electron Landau damping dominates or collisional damping dominates. Thus there is only a limited range of phase energies for which photoelectrons are the dominant contribution to the plasma line.

Figure 6 summarizes a set of plasma line data taken at Arecibo Observatory in February 27, 1977. The Arecibo Observatory is part of the National Astronomy and Ionosphere Center, which is operated by Cornell University under contract with the National Science Foundation. The plasma line measurements were interleaved with measurement of electron and ion temperatures and electron densities. We note that the anisotropy in plasma line temperatures shown in this data is typical of the 20-50% enhancement of T_p^+ over T_p^- found at Arecibo. Uncertainties in the data points are small and arise only through calibration uncertainties. During the nighttime, the asymmetry in the upshifted and downshifted plasma lines disappears. Superimposed on the figure are the measured values of ν_R.

RESULTS

The approach we have taken is to calculate the magnitude and pitch angle anisotropy of the photoelectron distribution function from the detailed transport equation and then derive the plasma line temperature we would observe. In this way we do not expect the calculation to be restricted to high altitudes or a particular range of phase energies. Figure (7) shows calculations of T_p^+ and T_p^- made with the photoelectron distribution function, $F(z,v,\mu)$, and Equations (9) through (20). The values of ν_R superimposed in the profiles were determined by electron temperatures and densities measured at Arecibo Observatory.

Figure (8) graphically summarizes the important terms contributing to Equation (7). Below about 200 km, f_p^- is greater than f_p^+, indicating a small anisotropy in electron flux: more electrons are going down than up. However in this region T_p is determined primarily by a balance between the source term, f_p, and the loss term, L_p. From Figure (8) we see that up to about 200 km,

$$\frac{L_p^-}{L_p^+} > \frac{f_p^-}{f_p^+}$$

indicating that the relative difference between L_p^+ and L_p^- is greater than that between f_p^+ and f_p^-. In Figure (9) we have rewritten the terms in the denominator of Equation (9) in terms of damping rates.

At high altitudes, f_p^+ is considerably larger than f_p^- and these remain the important source terms until about 400 km. The increasing importance of the damping due to thermal electrons tends to reduce the importance of the difference between L_p^+ and L_p^-. Up to that altitude where thermal electrons are dominant and when E_ϕ is very low, T_p^+ is greater than T_p^-.

An important point we wish to make is that previous calculations of the source and loss terms due to photoelectrons treat photoelectrons with velocities less than v_ϕ as Maxwellian. We note that especially at low altitudes the calculated photoelectron distribution function deviates strongly from Maxwellian at energies of a few ev. At altitudes below 200 km, our calculations indicate that 50-75% of L_p and 25-50% of f_p is evaluated in the integral range v_{min} to v_ϕ.

CONCLUSION

The investigations we have made of the photoelectron flux in the ionosphere have uncovered an anisotropy in the low altitude, low energy electron flux spectra. This arises through the conversion of a spatial inhomogeneity in the neutral atmosphere into a velocity distribution

anisotropy. The key to this is the forward peaked property of the elastic electron-neutral cross sections. We conclude that the downgoing electron flux is slightly larger than the upgoing flux in the altitude range from about 130 to 200 km.

In the altitude range described above, the plasma line amplitude is a balance between a source term f_p, which excites plasma waves to characteristic temperatures appropriate for photoelectrons, and a Landau damping term L_p. Our calculations show that the low energy photoelectrons ($E < E_\phi$) play a significant role in the damping. Treating them as Maxwellian severely underestimates their density and neglects their anisotropy.

ACKNOWLEDGMENTS

The authors would like to thank Dr. Jack Davis and Dr. J.C.G. Walker for their help and encouragement. This work is funded in part by the Naval Research Laboratory and the Office of Naval Research and in part by the National Astronomy and Ionosphere Center.

REFERENCES

Blaha, M., and J. Davis, Elastic Scattering of Electrons by Oxygen and Nitrogen at Intermediate Energies, *Phys. Rev. A*, 2319-2324, 1975.

Budden, K., *Radio Waves in the Ionosphere*, Cambridge University Press, Cambridge, 1966

Fremouw, E.J., J. Petriceks, and F.W. Perkins, Thomson Scatter Measurements of Magnetic Field Effects on the Landau Damping and Excitation of Plasma Waves, *Phys. Fluids*, **12**, 869-874, 1969.

Lejeune, G. and W. Kofman, Photoelectron Distribution Determination from Plasma Line Intensity Measurements Obtained at Nancy (France), *Planet. Space Sci.*, **25**, 123-133, 1977.

Oran, E., and D.J. Strickland, Calculation of the Ionospheric Photoelectron Distribution Function, NRL Memorandum Report 3361, 1976.

Perkins, F.W., E.E. Salpeter, K.O. Yngvesson, Incoherent Scatter from Plasma Oscillations in the Ionsophere, *Phys. Rev. Letters*, **14**, 579-581, 1965a.

Perkins, Francis and E.E. Salpeter, Enhancement of Plasma Density Fluctuations by Nonthermal Electrons, *Phys. Rev.*, **139A**, 555-62, 1965b.

Salpeter, E.E., Plasma Density Fluctuations in a Magnetic Field, *Phys. Rev.* **122**, 1663-1674, 1961.

Strickland, D.J., D.L. Book, T.P. Coffey, and J.A. Fedder, Transport Equation Techniques for the Deposition of Auroral Electrons, *J. Geophys. Res.*, **81**, 2755, 1976.

Yngvesson, K.O., and F.W. Perkins, Radar Thomson Studies of Photoelectrons in The Ionosphere and Landau Damping, *J. Geophys. Res.*, **73**, 97-110, 1968.

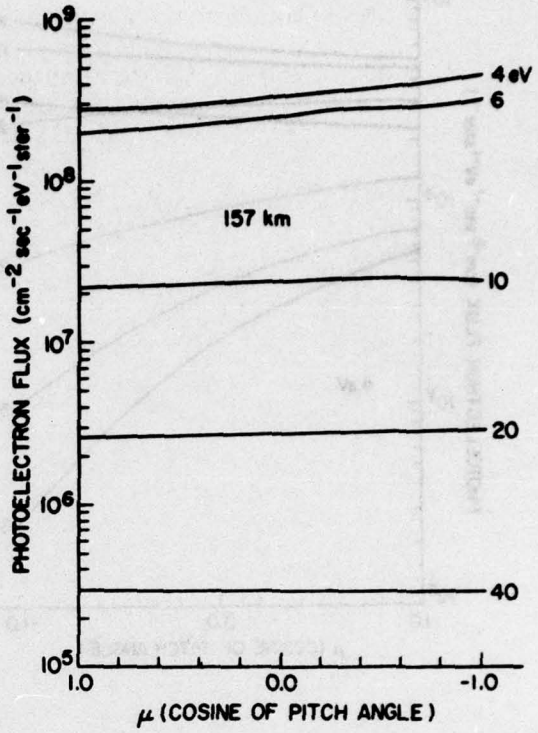

Fig. 1 — Calculated photoelectron flux as a function of μ, the cosine of the pitch angle, for selected energies at 157 km.

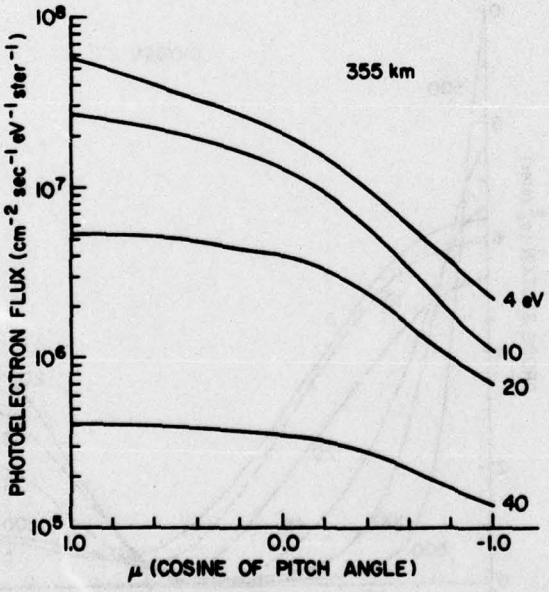

Fig. 2 — Calculated photoelectron flux as a function of pitch angle at 355 km.

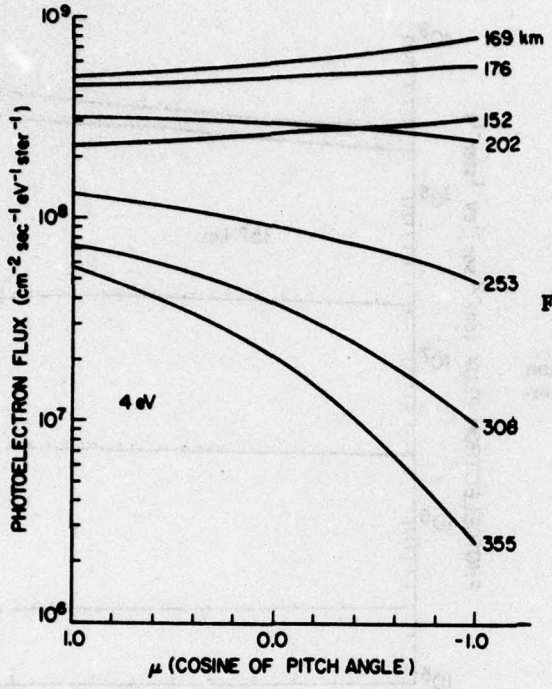

Fig. 3 — Calculated photoelectron flux at 4 ev as a function of pitch angle at selected altitudes.

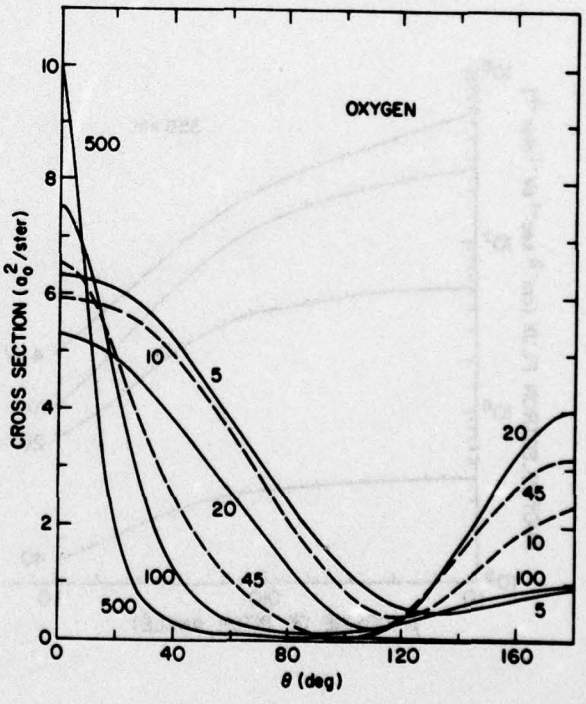

Fig. 4 — Differential cross sections for elastic scattering of electrons on the ground state of atomic oxygen (Blaha and Davis, 1975). The labels represent energies in ev.

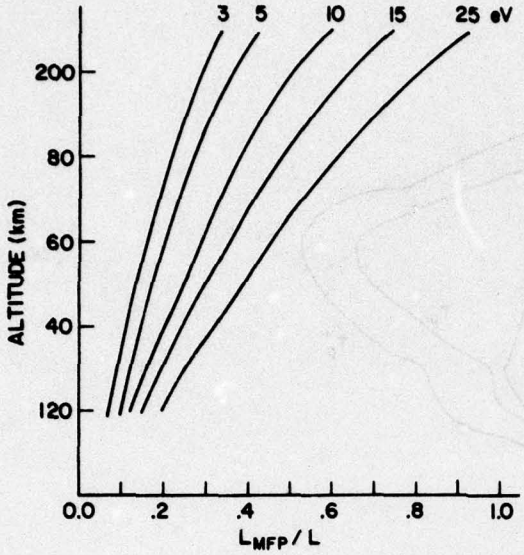

Fig. 5 — Ratio of the mean free path of electrons with energies between 3 and 25 ev to the neutral density scal height as a function of altitude.

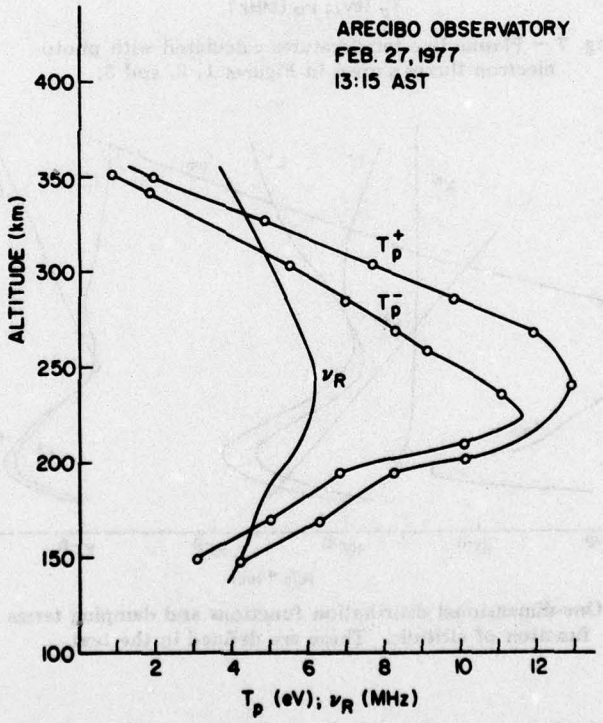

Fig. 6 — Plasma line temperatures and frequency measured at Arecibo Observatory.

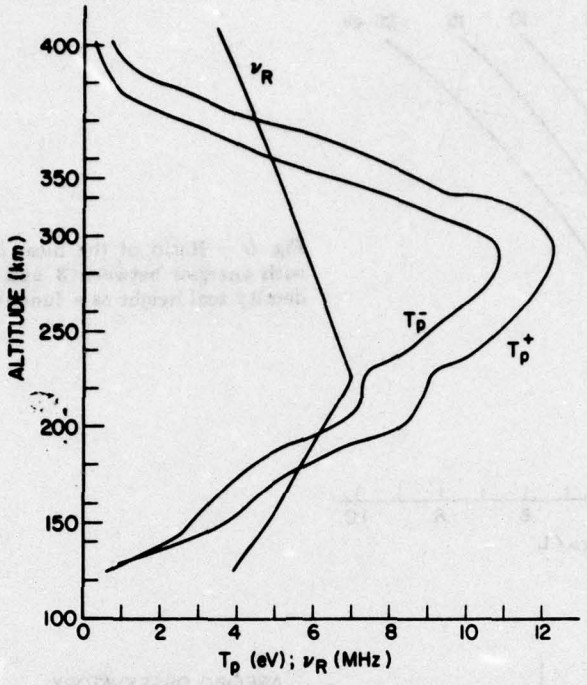

Fig. 7 — Plasma line temperatures calculated with photoelectron fluxes shown in Figures 1, 2, and 3.

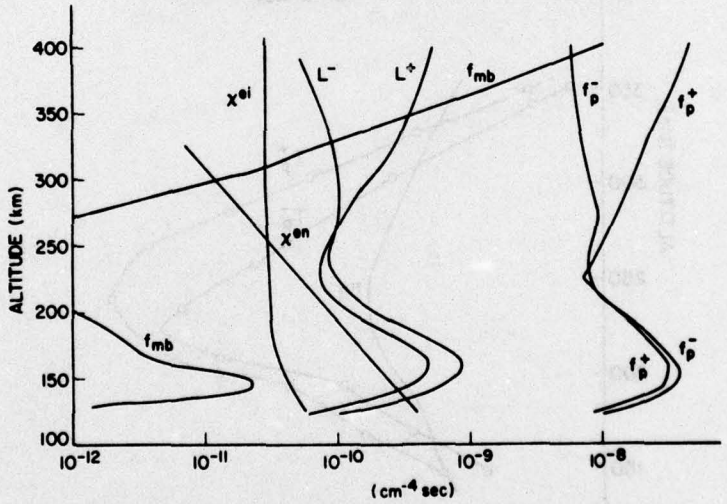

Fig. 8 — One-dimensional distribution functions and damping terms as a function of altitude. These are defined in the text.

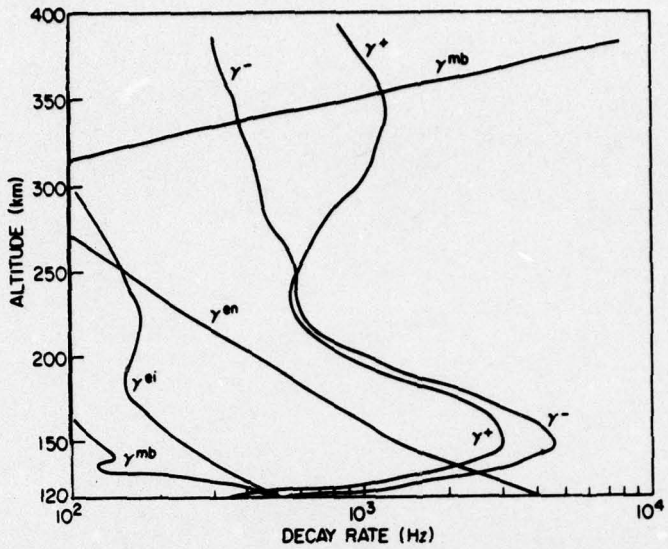

Fig. 9 — Damping rates due to electron ion and electron neutral collisions (λ^{ei} and λ^{en}), collisions with the ambient electron gas λ^{mb}, and excitation of plasma waves ($\lambda^{\pm}$).